Published in final edited form as:
ACS Chem Biol. 2011 June 17; 6(6): 628–635. doi:10.1021/cb100428c.

Identification of specific inhibitors of human RAD51 recombinase using high-throughput screening

Fei Huang[1], **Nuzhat A. Motlekar**[2], **Chelsea M. Burgwin**[1], **Andrew D. Napper**[2], **Scott L. Diamond**[2,3], and **Alexander V. Mazin**[1,*]

[1] Department of Biochemistry and Molecular Biology, Drexel University College of Medicine, Philadelphia, PA 19102, USA

[2] Penn center for Molecular Discovery, University of Pennsylvania, Philadelphia, PA 19102, USA

[3] Department of Genetics, University of Pennsylvania, Philadelphia, PA 19104, USA

Abstract

RAD51 is a key protein of homologous recombination that plays a critical role in the repair of DNA double-strand breaks (DSB) and interstrand cross links (ICL). To better understand the cellular function(s) of human RAD51, we propose to develop specific RAD51 inhibitors. RAD51 inhibitors may also help to increase the potency of anticancer drugs that act by inducing DSBs or ICLs, e.g., cisplatin or ionizing radiation. *In vitro,* RAD51 promotes DNA strand exchange between homologous ss- and dsDNA. Here, we developed a DNA strand exchange assay based on fluorescence resonance energy transfer and used this assay to identify RAD51 inhibitors by high throughput screening of the NIH Small Molecule Repository (>200,000 compounds). Seventeen RAD51 inhibitors were identified and analyzed for selectivity using additional non-fluorescent DNA-based assays. As a result, we identified a compound (**B02**) that specifically inhibited human RAD51 (IC_{50} = 27.4 μM), but not its *E. coli* homologue RecA (IC_{50} > 250 μM). Two other compounds (A03 and A10) were identified that inhibited both RAD51 and RecA, but not the structurally unrelated RAD54 protein. The structure-activity relationship (SAR) analysis allowed us to identify the structural components of **B02** that are critical for RAD51 inhibition. The described approach can be used for identification of specific inhibitors of other human proteins that play an important role in DNA repair, e.g., RAD54 or Bloom's syndrome helicase.

Keywords

homologous recombination; RAD51; DNA strand exchange; small molecule inhibitors; high throughput screening

INTRODUCTION

Homologous recombination plays a critical role in the repair of DNA double-strand breaks (DSBs) and interstrand crosslinks (ICL), the most harmful types of DNA lesions (1–3). DSBs are induced by various chemical agents and ionizing radiation. DSBs also form during the repair of ICLs. Once DSB are formed, they are processed first by exonucleases to

*Corresponding Author: Alexander Mazin, Ph. D., Drexel University College of Medicine, Department of Biochemistry and Molecular Biology, 245 N 15th Street, MS 497, NCB, Room 10103, Philadelphia, PA 19102–1192, Tel: 215–762–7195; Fax: 215–762–4452, amazin@drexelmed.edu.

Subject Categories: DNA replication, repair, recombination, and chromosome dynamics

Supporting Information Available: This material is available free of charge *via* the Internet.

generate extensive ssDNA tails (4, 5). Then RAD51 protein binds these ssDNA tails forming helical nucleoprotein filaments that promote a search for homologous dsDNA sequences (6). Once homologous dsDNA sequences are found, RAD51 promotes DNA strand exchange between the ssDNA that resides within the filament and homologous dsDNA, i.e., an invasion of ssDNA into homologous DNA duplex that results in the displacement of the identical ssDNA from the duplex and formation of a joint molecule. Joint molecules, key intermediates of DSB repair, provide both the template and the primer for DNA repair synthesis that is required for DSB repair (7).

By promoting DNA strand exchange RAD51 plays a key role in homologous recombination. The protein is evolutionarily conserved from bacteriophages to mammals; in all organisms RAD51 orthologs play an important role in DNA repair and homologous recombination (3, 8–10). However, only in higher eukaryotes does Rad51 become essential for cell viability. The knockout of the murine *RAD51* gene caused embryonic lethality of homozygotes (11). Murine embryonic fibroblasts became prematurely senescent in tissue culture and did not proliferate for more than a few generations. Rad51 inactivation is detrimental for proliferation of the chicken DT-40 cells, as well (12).

Because homologous recombination plays an important role in the repair of DSBs and ICLs, it was proposed that the efficiency of traditional anti-cancer therapies, which widely use ionizing radiation and other DSB- and ICL-inducing agents, can be increased by inhibiting homologous recombination in cancer cells (13). Because RAD51 plays a key role in homologous recombination, we suggest that identification and use of RAD51 inhibitors may lead to development of novel combination anti-cancer therapies. RAD51 was found to be overexpressed in many tumors including familial BRCA1-deficient breast tumors (14–16). It is though that overexpression of RAD51 rescues homologous recombination by compensating for the lack of functional BRCA1 or other DNA repair proteins. Because RAD51 overexpression may contribute to chemo- and radioresistance of human cancers (17), this protein may represent an important target for anti-cancer therapy. Also, the inhibitors that block specific activities of RAD51, like DNA strand exchange or ATP hydrolysis, may help to investigate the cellular functions of this protein.

In order to identify specific RAD51 inhibitors, we used an efficient high throughput screening (HTS) of chemical compound libraries. To carry out HTS, we developed an assay based on fluorescence resonance energy transfer (FRET). By screening ~200,000 compounds from the NIH Small Molecule Repository we identified seventeen compounds that inhibited RAD51 DNA strand exchange activity. We further examined these compounds using a secondary non-fluorescent DNA strand exchange assay, known as a D-loop assay (18, 19). This assay confirmed the inhibitory effect of eleven selected compounds and identified four compounds as the most potent RAD51 inhibitors. Further analysis allowed us to identify a compound (**B02**) that selectively inhibited human RAD51, but not *E. coli* RecA ortholog. In addition, two other compounds (**A03 and A10**) were identified as inhibitors of RAD51 and RecA, but not the structurally unrelated RAD54 protein (20). Finally, we carried out inhibitor optimization and performed a structure-activity relationships (SARs) analysis of the **B02** inhibitor.

RESULTS AND DISCUSSION

A fluorescence-based DNA strand exchange assay

Here, we developed a FRET-based DNA strand exchange assay suitable for HTS of large libraries of chemical compounds. In this assay, RAD51 promotes DNA strand exchange between homologous synthetic ssDNA and dsDNA substrates. The dsDNA carries fluorescein (FLU), a fluorescent donor group, and black hole quencher 1 (BHQ1), a non-

fluorescent acceptor group, which were attached to the 5′- and 3′-ends of the complementary ssDNA strands, respectively (Figure 1A). In this dsDNA substrate, the fluorescence of the FLU group is quenched by BHQ1 through FRET. As a result of RAD51-promoted DNA strand exchange, the FLU-carrying DNA strand is displaced from the dsDNA that carries the BHQ1 and the fluorescence of the FLU group increases (21, 22).

Using this assay we measured the kinetics of RAD51-promoted DNA strand exchange. RAD51 was loaded on the homologous ssDNA (Oligo 25; 48-mer) (denoted as "Homologous DNA") to form the nucleoprotein filament. Then, fluorescently labeled dsDNA (Oligo 25-FLU and 26-BHQ1) was added to the filament to initiate DNA strand exchange. We found that after a 1 h incubation the fluorescence intensity at 521 nm increases approximately 20–fold (Figure 1B). To ensure that the observed fluorescence increase resulted from DNA strand exchange we carried out a control in which the RAD51 filament was assembled on heterologous ssDNA (Oligo 374, 48-mer) (denoted as "Heterologous DNA"). Since DNA strand exchange does not occur between heterologous DNA molecules (19), no increase in fluorescence was expected. Indeed, in the case of heterologous DNA the intensity of fluorescence remained almost constant during the 1 h of incubation (Figure 1B). Thus, the results validated the FRET-based assay to measure the DNA strand exchange activity of RAD51.

HTS of the NIH Small Molecule Repository

The NIH Small Molecule Repository (202,556 compounds) was screened for RAD51 inhibitors using the FRET-based assay described above. 174 positive hits that showed more than 30% inhibition of the DNA strand exchange activity of RAD51were detected (hit rate, 0.09%) using a Perkin Elmer Envision 2102 multilabel reader. Measuring the concentration dependence of RAD51 inhibition by these compounds allowed us to identify the seventeen most potent inhibitors as candidates that warranted further analysis (Figure 2).

Analysis of RAD51 inhibitors using the D-loop assay

To validate the hits identified in the primary FRET-based assay, the seventeen selected compounds (Figure 2) were further analyzed using the D-loop assay. In the D-loop assay, DNA strand exchange was promoted by RAD51 between homologous ^{32}P-labeled ssDNA and pUC19 supercoiled plasmid DNA (Figure 3a) (18). The products of this reaction, joint molecules, also known as D-loops (called after the displaced DNA strand that is formed in joint molecules during DNA strand exchange), were identified by electrophoresis in a 1% agarose gel. First, we measured the inhibitory effect each of the seventeen compounds had on the efficiency of D-loop formation. We found that eleven of the seventeen compounds inhibited D-loop formation by more than 50% (Figure 3b, c; Supplementary Table 1). Thus, 65% of the compounds identified in the primary assay were validated by the secondary assay. In addition, we found using a fluorescence intercalator (ethidium bromide) displacement assay that **A05, A06, A14**, and **A15** were DNA binders (data not shown). These compounds along with **A08, A11**, and **B01**, which showed relatively modest inhibition, were not analyzed further. Then, we determined the IC_{50} values for the four most potent remaining inhibitors of the RAD51 DNA strand exchange activity using the D-loop assay. The IC_{50} for **A03, A04, A10**, and **B02** were 33.2 μM, 5.0 μM, 26.6 μM, and 27.4 μM, respectively (Figure 4; Supplementary Table 2).

Specificity of the RAD51 inhibitors

RAD51 shares structural and functional similarity with RecA from *E. coli*; both proteins promote DNA strand exchange *in vitro* and share 30% homology (10, 23, 24). Using the D-loop assay we wished to determine the effect of the selected RAD51 inhibitors on the DNA strand exchange activity of RecA. We found that **A03** showed some moderate specificity for

RAD51 (Figure 5a), with the IC_{50} 5.6–fold lower for RAD51 than for RecA (Supplementary Table 2). The **A04** and **A10** compounds inhibited RAD51 and RecA with a nearly equal efficiency (Figure 5b, c; Supplementary Table 2). Finally, **B02** showed the highest specificity for RAD51 (Figure 5d); the IC_{50} for RAD51 was 27.4 μM, whereas for RecA we did not observe any significant inhibition of DNA strand exchange up to 250 μM of **B02** (Supplementary Table 2).

We next tested whether the inhibitory effects of **A03, A04**, and **A10** compounds were specific for the proteins of the Rad51/RecA family or they have a broader specificity. To address this question we tested the effect of the inhibitors on human RAD54, a Swi2 protein, which does not share structural homology with the proteins of the RecA/RAD51 family (20). RAD54 promotes branch migration of Holliday junctions, a process in which one DNA strand is progressively exchanged for another (Figure 6a) (25, 26). We tested the effect of **A03, A04, A10, and B02** compounds on the RAD54 branch migration activity using a ^{32}P-labeled oligonucleotide-based cruciform DNA substrate, known as the partial Holliday junction or PX-junction (Figure 6a) (25). Of the four compounds tested, we found that **A03, A10,** and **B02** did not significantly inhibit RAD54 in the range of concentrations from 0 to 200 μM (Figure 6b). However, **A04** did have an inhibitory effect on the RAD54 branch migration activity (IC_{50} = 2.6 μM) (Figure 6c).

Thus among tested compounds, **B02** was identified as a specific inhibitor of human RAD51. **A03** and **A10** inhibited both RAD51/RecA family proteins, RAD51 and RecA; **A04** showed the broadest inhibitory spectrum by inhibiting all three tested proteins: RAD51, RecA, and RAD54.

SAR analysis of B02 inhibitor

For SAR analysis of **B02** we set up a 16-compound library of **B02** derivatives (Figure 7A). According to the structural features, the 16 compounds were sorted in 5 groups. In group 1(compound **B02-1**): (*E*)-2-(pyridin-3-yl) vinyl was removed; in group 2 (compounds **B02-2a-2h**): (*E*)-2-(pyridin-3-yl) vinyl was replaced with (*E*)-2-(R_1-substituting group) vinyl; in group 3 (compounds **B02-3a-3e**): benzyl was replaced with R_2; in group 4 (compound **B02-4**): the core, quinazolin-4(*3H*)-one was replaced by 6-iodo-quinazolin-4(*3H*)-one; in group 5 (compound **B02-5**): the core, quinazolin-4(*3H*)-one was replaced by 6-iodo-quinazolin-4(*3H*)-one, as well as (*E*)-2-(pyridin-3-yl) vinyl was replaced by (*E*)-2-(pyridin-2-yl) vinyl.

The inhibitory effect of these **B02** derivatives (50 μM) on the DNA strand exchange activity of RAD51was determined using the D-loop assay. We found that the only position of BO2 that could tolerate modifications and still inhibit RAD51 was the benzyl (compound group 3) (Figure 7B and 7C). Moreover, only **B02-3a** (R_2 = ethyl) and **B02-3b** (R_2 = *m*-methyl phenyl) retain the inhibitory effect, the substitutions of other groups (**B02-3d**, R_2 = phenyl and **B02-3e**, R_2= methyl) or at the different positions (**B02-3c**, R_2 = *p*-methyl phenyl) eliminates the inhibition, suggesting that the inhibition is tightly related to the size and the steric conformation of the substituting group. All other tested replacements in the groups 1, 2, 4, and 5 eliminated RAD51 inhibition. The high sensitivity of the RAD51 inhibition to **B02** modifications suggests specific interactions between the inhibitor molecule and RAD51 protein.

Inhibitor optimization

From the library of **B02** derivatives, two compounds (**B02-3a** and **B02-3b**) that inhibited RAD51 were identified (Figure 7). For these two inhibitors, the IC_{50} values of the RAD51 DNA strand exchange activity and their selectivity for RAD51 were determined using the D-

loop assay (Figure 8). The IC_{50} for **B02-3a** and **B02-3b** are 15.3 μM and 27.3 μM, respectively (Figure 8B, C). To evaluate the selectivity of the inhibitors we tested the effect of **B02-3a** and **B02-3b** on the DNA strand exchange activity of RecA. The results show that **B02-3a** and **B02-3b** in concentrations up to 100 μM do not inhibit RecA (Figure 8; Supplementary Table 2).

Thus, the current results demonstrate the feasibility and efficiency of the HTS approach for discovery of novel selective inhibitors of RAD51, a key protein of homologous recombination and the repair of DNA double strand breaks and interstrand crosslinks. Further experiments that are currently in progress (Huang et. al., unpublished data) will establish the mechanism of specific RAD51 inhibition by selected small molecule compounds (**B02, A03, A10**) and examining the effect of these compounds on the RAD51-dependent homologous recombination and DNA repair in human cells.

METHODS

Proteins and DNA

RecA was purchased from USB Inc. Human RAD51 and RAD54 were purified as described (27) (28). The oligonucleotides used in this study (Supplementary Table 3) were purchased from IDT Inc. in a desalted form. Oligonucleotide and pUC19 DNA substrates were prepared as described (29, 30). The DNA concentrations are expressed as moles of nucleotide.

Compound libraries

We used the NIH Small Molecule Repository (202,556 compounds) for the primary screening for RAD51 inhibitors. All the compounds were dissolved in DMSO (Sigma, Cat # D8418); concentrations of stock solutions were 2.5 mM or 5 mM. In the working solutions the DMSO concentration added with the stock of compounds was 2% (v/v), unless indicated otherwise. The compounds for SAR analysis were purchased from Chembridge Co.

The fluorescence-based DNA strand exchange assay

To measure the RAD51 DNA strand exchange activity, we developed a fluorescence-based assay. In this assay, dsDNA substrate was prepared by annealing two complementary ssDNA oligonucleotides Oligos 25-FLU and 26-BHQ1. Oligo 25-FLU contains the fluorescein group, a donor fluorophore with the excitation maximum at 490 nm and the emission maximum at 521 nm, at the 5′-end. Oligo 26-BHQ1 contains the black hole quencher 1 (BHQ1), a non-fluroescent acceptor, at the 3′-end. To form the nucleoprotein filament, RAD51 (200 nM) was incubated with a 48-mer ssDNA (Oligo 25) (600 nM, nt) in DNA strand exchange buffer containing 40 mM Tris-HCl (pH 7.8), 2 mM ATP, 5 mM $CaCl_2$, 1 mM DTT and 100 μg ml^{-1} BSA for 15 min at 37 °C. DNA strand exchange was initiated by addition of dsDNA (600 nM, nt) (Oligos 25-FLU and 26-BHQ1). Previously, it was shown that Ca^{2+}, strongly stimulates DNA strand exchange activity of RAD51, but not that of the yeast and bacterial RAD51 homologues (18). The reactions were carried out for indicated period of time at 37 °C or 23 °C, as indicated. The fluorescence intensity was measured using a Fluoromax3 fluorimeter (Jobin Yvon).

HTS of the NIH SMR for RAD51 inhibitors

To form the nucleoprotein filament, RAD51 (300 nM) was incubated with a 48-mer ssDNA (Oligo 25) (600 nM, nt) in DNA strand exchange buffer containing 40 mM HEPES (pH 7.8), 2 mM ATP, 5 mM $CaCl_2$, 1 mM DTT and 100 μg ml^{-1} BSA for 15 min at 37 °C. 10 μl aliquots of the mixtures were added to the plates containing the NIH Small Molecule Repository and further incubated at 23 °C for 30 min. DNA strand exchange reactions were

initiated by addition of dsDNA (300 nM, nt) (Oligos 25-FLU and 26-BHQ1) and carried out at 23 °C for 15 min, or otherwise indicated periods of time. Compound concentration was 8.5 μM, unless indicated otherwise, DMSO concentrations in wells was 1.7% (v/v). HTS of chemical compound libraries was performed in 384 or 1536 well plates using a Perkin Elmer Envision 2102 multilabel reader. The compounds with an inhibitory effect of 30% or greater were tested further by measuring the concentration dependence (in a range from 1 nM to 100 μM) of their inhibition of RAD51. The most potent inhibitory compounds were analyzed further using non-fluorecent assays.

The D-Loop assay for the RAD51

The D-loop assay was performed essentially as described previously (18). To form the nucleoprotein filament RAD51 protein (1 μM) was incubated with a ^{32}P-labeled 90 mer ssDNA (Oligo 90) (3 μM, nt) in buffer containing 25 mM Tris-acetate (pH 7.5), 1 mM ATP, 1 mM $CaCl_2$, 100 μg ml^{-1} BSA, 1 mM DTT and 20 mM KCl for 15 min at 37 °C. When indicated, chemical compounds in question were added in specified concentrations and incubation was continued for 30 min at 37 °C. D-loop formation was initiated by addition of supercoiled pUC19 dsDNA (50 μM, nt) and continued for 15 min. Reactions were stopped by addition of SDS to 1% (w/v) and proteinase K to 880 μg ml^{-1} followed by incubation for 15 min at 37°C. Samples were mixed with 0.1 vol of loading buffer (70% (v/v) glycerol, 0.1% (w/v) bromophenol blue) and analyzed by electrophoresis in 1% (w/v) agarose-TAE (40 mM Tris-acetate, pH 8.0 and 1 mM EDTA) gels. The yield of joint molecules was expressed as a percentage of the total plasmid DNA.

The D-Loop assay for RecA

To form the nucleoprotein filament RecA protein (1 μM) was incubated with a 90 mer ^{32}P-labeled ssDNA (Oligo 90) (3 μM, nt) in buffer containing 25 mM Tris-acetate (pH 7.5), 1 mM ATP, 10 mM $MgCl_2$, 100 μg ml^{-1} BSA, 1 mM DTT, 3 mM phosphoenolpyruvate and 5 U ml^{-1} pyruvate kinase for 5 min at 37 °C (31). When indicated, chemical compounds in specified concentrations were added and incubation was continued for 30 min at 37°C. D-loop formation was initiated by addition of supercoiled pUC19 dsDNA (50 μM, nt) and carried out for 3 min at 37 °C. The DNA products were deproteinized and analyzed as described above for the Rad51-promoted reaction.

The DNA branch migration assay for RAD54

The partial Holliday junction (PX-junction), in which one of the four DNA arms is single-stranded (Figure 6A), was used as a substrate for the 4-stranded branch migration promoted by RAD54 (26). PX junctions were constructed in such a way (by incorporating a region of heterology) that allowed branch migration only in one direction (25). To produce PX-junctions, tailed DNA (Oligos 170 and 171) (1.45 μM, molecules) was annealed with ^{32}P-labeled fork DNA (Oligos 71 and 169) (1.33 μM, molecules) in branch migration buffer containing 25 mM Tris acetate, pH 7.5, 3 mM magnesium acetate, 2 mM ATP, 1 mM dithiothreitol, 100 μg ml^{-1} bovine serum albumin, 10 U ml^{-1} creatine phosphokinase, 15 mM creatine phosphate for 10 min at 37 °C and then for 10 min at 30 °C. Then, branch migration was initiated immediately by addition of the RAD54 (100 nM) to PX-junctions (33 nM, molecules) in branch migration buffer and was carried out at 30 °C. Aliquots (10 μl) were withdrawn after 0, 3, 5, 15, 30, and 60 min. The DNA products were deproteinized by treatment with stop buffer (1.4% (w/v) SDS, 960 μg ml^{-1} proteinase K, 7.5% (w/v) glycerol, 0.015% (w/v) bromphenol blue) for 5 min at 22 °C and analyzed by electrophoresis in 8% (w/v) polyacrylamide gels (29:1) in 1 X TBE buffer (89 mM Tris borate, pH 8.3, and 1 mM EDTA) at 22 °C. The gels were dried on DE81 chromatography paper (Whatman) and quantified using a Storm 840 PhosphorImager (Molecular Dynamics).

Ethidium bromide displacement assay

Ethidium bromide (0.5 mg ml^{-1}) was added to pUC19 supercoiled dsDNA (2 μg ml^{-1}) in buffer containing 25 mM Tris acetate, pH 7.5, 20 mM NaCl, and 10 μM EDTA followed by 1 min incubation. The fluorescence of the sample was measured using a FlouroMax-3 fluorimeter at an excitation wavelength of 260 nm and an emission wavelength of 546 nm. Then, the small molecule inhibitors were added in increasing concentrations and allowed to equilibrate for 1 min, followed by the fluorescence measurement.

Calculation of the IC_{50} value for RAD51 inhibitors

IC_{50} values were calculated using GraphPad Prism V5.0 software and the sigmoidal dose-response function. The data were obtained from three independent repeats of experiments.

Supplementary Material

Refer to Web version on PubMed Central for supplementary material.

Acknowledgments

We thank Matthew Rossi, Olga Mazina, and members of the Diamond lab for comments and discussion. This work was supported by the NIH Grants CA100839, MH084119 (to AVM), U54-HG003915 (to SLD) and the Leukemia and Lymphoma Society Scholar Award 1054-09 (to AVM).

References

1. Helleday T, Lo J, van Gent DC, Engelward BP. DNA double-strand break repair: From mechanistic understanding to cancer treatment. DNA Repair (Amst). 2007
2. Krogh BO, Symington LS. Recombination proteins in yeast. Annu Rev Genet. 2004; 38:233–271. [PubMed: 15568977]
3. San Filippo J, Sung P, Klein H. Mechanism of eukaryotic homologous recombination. Ann Rev Biochem. 2008; 77:229–257. [PubMed: 18275380]
4. Cejka P, Cannavo E, Polaczek P, Masuda-Sasa T, Pokharel S, Campbell JL, Kowalczykowski SC. DNA end resection by Dna2-Sgs1-RPA and its stimulation by Top3-Rmi1 and Mre11-Rad50-Xrs2. Nature. 2010; 467:112–116. [PubMed: 20811461]
5. Mimitou EP, Symington LS. DNA end resection: many nucleases make light work. DNA Repair (Amst). 2009; 8:983–995. [PubMed: 19473888]
6. Kowalczykowski SC. Structural biology: snapshots of DNA repair. Nature. 2008; 453:463–466. [PubMed: 18497811]
7. Pâques F, Haber JE. Multiple pathways of recombination induced by double-strand breaks in Saccharomyces cerevisiae. Microbiol Mol Biol Rev. 1999; 63:349–404. [PubMed: 10357855]
8. Bianco PR, Tracy RB, Kowalczykowski SC. DNA strand exchange proteins: a biochemical and physical comparison. Front Biosci. 1998; 3:D570–603. [PubMed: 9632377]
9. Brendel V, Brocchieri L, Sandler SJ, Clark AJ, Karlin S. Evolutionary comparisons of RecA-like proteins across all major kingdoms of living organisms. J Mol Evol. 1997; 44:528–541. [PubMed: 9115177]
10. Lin Z, Kong H, Nei M, Ma H. Origins and evolution of the recA/RAD51 gene family: evidence for ancient gene duplication and endosymbiotic gene transfer. Proc Natl Acad Sci USA. 2006; 103:10328–10333. [PubMed: 16798872]
11. Lim DS, Hasty P. A mutation in mouse rad51 results in an early embryonic lethal that is suppressed by a mutation in p53. Mol Cell Biol. 1996; 16:7133–7143. [PubMed: 8943369]
12. Sonoda E, Sasaki MS, Buerstedde JM, Bezzubova O, Shinohara A, Ogawa H, Takata M, Yamaguchi-Iwai Y, Takeda S. Rad51-deficient vertebrate cells accumulate chromosomal breaks prior to cell death. EMBO J. 1998; 17:598–608. [PubMed: 9430650]

13. Helleday T. Homologous recombination in cancer development, treatment and development of drug resistance. Carcinogenesis. 2010; 31:955–960. [PubMed: 20351092]
14. Raderschall E, Stout K, Freier S, Suckow V, Schweiger S, Haaf T. Elevated levels of Rad51 recombination protein in tumor cells. Cancer Res. 2002; 62:219–225. [PubMed: 11782381]
15. Xia SJ, Shammas MA, Shmookler Reis RJ. Elevated recombination in immortal human cells is mediated by HsRAD51 recombinase. Mol Cell Biol. 1997; 17:7151–7158. [PubMed: 9372947]
16. Maacke H, Opitz S, Jost K, Hamdorf W, Henning W, Kruger S, Feller AC, Lopens A, Diedrich K, Schwinger E, Sturzbecher HW. Over-expression of wild-type Rad51 correlates with histological grading of invasive ductal breast cancer. International Journal of Cancer. 2000; 88:907–913.
17. Ito M, Yamamoto S, Nimura K, Hiraoka K, Tamai K, Kaneda Y. Rad51 siRNA delivered by HVJ envelope vector enhances the anti-cancer effect of cisplatin. The journal of gene medicine. 2005; 7:1044–1052. [PubMed: 15756713]
18. Bugreev DV, Mazin AV. Ca2+ activates human homologous recombination protein Rad51 by modulating its ATPase activity. Proc Natl Acad Sci USA. 2004; 101:9988–9993. [PubMed: 15226506]
19. Shibata T, DasGupta C, Cunningham RP, Radding CM. Purified Escherichia coli recA protein catalyzes homologous pairing of superhelical DNA and single-stranded fragments. Proc Natl Acad Sci USA. 1979; 76:1638–1642. [PubMed: 156361]
20. Mazin AV, Mazina OM, Bugreev DV, Rossi MJ. Rad54, the motor of homologous recombination. DNA Repair (Amst). 2010; 9:286–302. [PubMed: 20089461]
21. Parkhurst KM, Parkhurst LJ. Donor-acceptor distance distributions in a double-labeled fluorescent oligonucleotide both as a single strand and in duplexes. Biochemistry. 1995; 34:293–300. [PubMed: 7819210]
22. Parkhurst LJ, Parkhurst KM, Powell R, Wu J, Williams S. Time-resolved fluorescence resonance energy transfer studies of DNA bending in double-stranded oligonucleotides and in DNA-protein complexes. Biopolymers. 2001; 61:180–200. [PubMed: 11987180]
23. Baumann P, Benson FE, West SC. Human Rad51 protein promotes ATP-dependent homologous pairing and strand transfer reactions in vitro. Cell. 1996; 87:757–766. [PubMed: 8929543]
24. Ogawa T, Yu X, Shinohara A, Egelman EH. Similarity of the yeast RAD51 filament to the bacterial RecA filament. Science. 1993; 259:1896–1899. [PubMed: 8456314]
25. Bugreev DV, Mazina OM, Mazin AV. Rad54 protein promotes branch migration of Holliday junctions. Nature. 2006; 442:590–593. [PubMed: 16862129]
26. Mazina OM, Rossi MJ, Thomaa NH, Mazin AV. Interactions of human rad54 protein with branched DNA molecules. J Biol Chem. 2007; 282:21068–21080. [PubMed: 17545145]
27. Sigurdsson S, Trujillo K, Song B, Stratton S, Sung P. Basis for avid homologous DNA strand exchange by human Rad51 and RPA. J Biol Chem. 2001; 276:8798–8806. [PubMed: 11124265]
28. Mazina OM, Mazin AV. Human Rad54 protein stimulates DNA strand exchange activity of hRad51 protein in the presence of Ca2+ J Biol Chem. 2004; 279:52042–52051. [PubMed: 15466868]
29. Bugreev DV, Mazina OM, Mazin AV. Analysis of branch migration activities of proteins using synthetic DNA substrates. Nature Protocols. 2006 published online 1 September 2006 (doi: 2010.1038/nprot.2006.2217).
30. Rossi MJ, Mazina OM, Bugreev DV, Mazin AV. Analyzing the branch migration activities of eukaryotic proteins. Methods. 51:336–346. [PubMed: 20167275]
31. Mazin AV, Zaitseva E, Sung P, Kowalczykowski SC. Tailed duplex DNA is the preferred substrate for Rad51 protein-mediated homologous pairing. EMBO J. 2000; 19:1148–1156. [PubMed: 10698955]

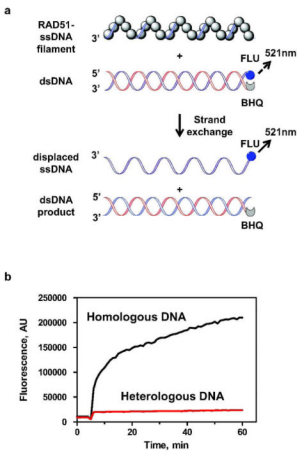

Figure 1. Measuring RAD51-promoted DNA strand exchange using the FRET-based assay

(A) The reaction scheme. FLU and BHQ denote fluorescein and black hole quencher 1, respectively. Broken- and solid-line arrows denote fluorescein emission at 521 nm before and after DNA strand exchange, respectively. The excitation wavelength was 490 nm. (B) The kinetics of DNA strand exchange promoted by RAD51. The fluorescence intensity was expressed in arbitrary units (AU). “Homologous DNA” and “Heterologous DNA” denote reactions with homologous (Oligo 25, 48-mer) and heterologous ssDNA (Oligo 374, 48-mer), respectively.

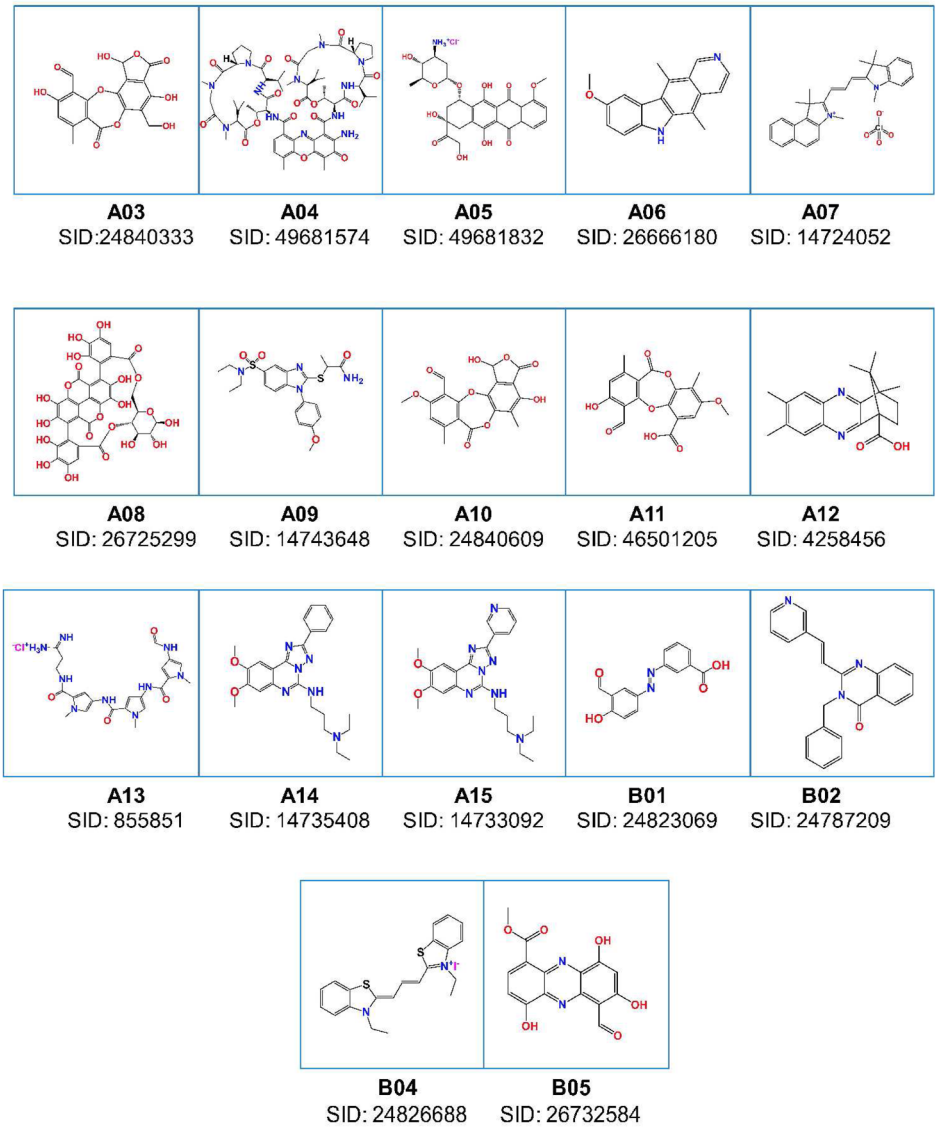

Figure 2. The RAD51 inhibitors identified by HTS

"SID" indicate substance ID (http://pubchem.ncbi.nlm.nih.gov/).

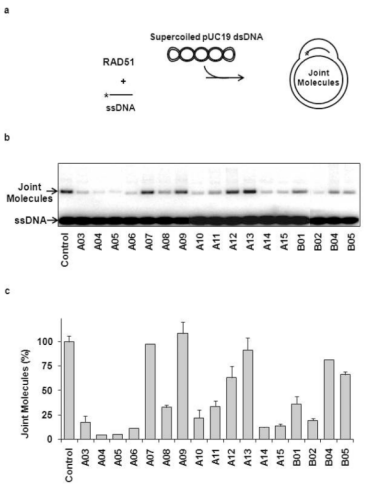

Figure 3. Secondary screening of the RAD51 inhibitors using the D-loop assay

(A) The scheme of D-loop formation promoted by RAD51. The asterisk denotes the ^{32}P label. (B) Analysis of 17 compounds selected by HTS. RAD51 (1 μM) was incubated with a 90-mer ssDNA (3 μM) (Oligo 90) to form the filament followed by addition of indicated compounds (100 μM). Joint molecule (D-loop) formation was initiated by addition of pUC19 supercoiled dsDNA (50 μM). The DNA products were analyzed by electrophoresis in a 1% agarose gel. The control was carried out under identical conditions except that no tested compounds were added. (C) The effect of selected compounds on the yield of joint molecules was plotted as a graph. The extent of D-loop formation in the absence of inhibitors, 40.3%, was expressed as 100% of D-loop formation efficiency. Experiments were repeated at least three times; error bars represent S.D. (standard deviation).

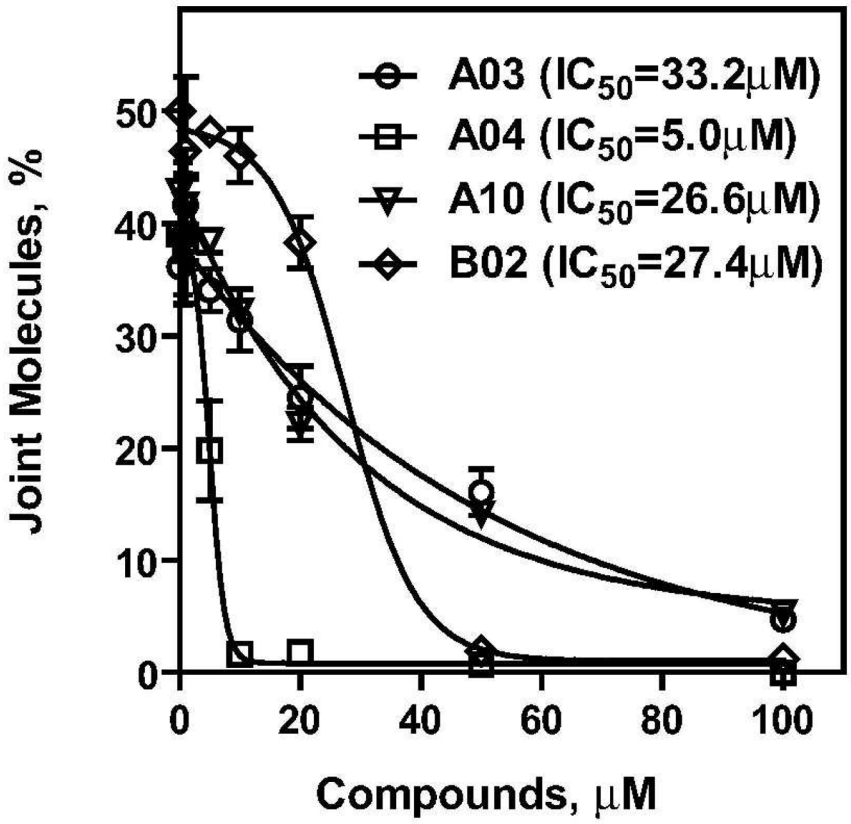

Figure 4. The IC_{50} of RAD51 inhibition by four selected compounds determined in the D-loop assay

RAD51 (1 μM) was incubated with a 90-mer ssDNA (3 μM) (Oligo 90) to form the filament followed by addition of **A03, A04, A10**, and **B02** inhibitors in indicated concentrations. After a 30-min incubation, D-loop formation was initiated by addition of pUC19 supercoiled dsDNA (50 μM). The DNA products were analyzed by electrophoresis in a 1% agarose gel. Experiments were repeated at least three times; error bars represent S.D.

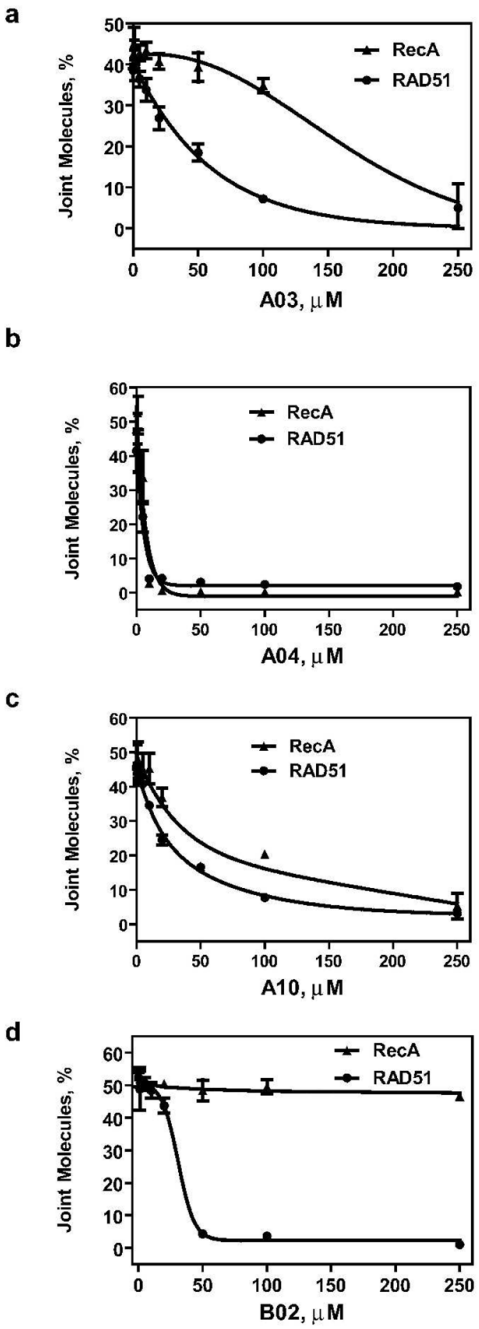

Figure 5. Specificity of RAD51 inhibition by A03, A04, A10, and B02 compounds

RAD51 (1 μM) or RecA (1 μM) was incubated with a 90-mer ssDNA (3 μM) (Oligo 90) for 15 min (for RAD51) or 5 min (for RecA) to form the nucleoprotein filament. Then tested compounds in indicated concentrations were added and incubation continued for 30 min. The D-loop formation was initiated by addition of pUC19 supercoiled dsDNA (50 μM) and continued for 15 min (for RAD51) or 3 min (for RecA). The DNA products were analyzed by electrophoresis in a 1% agarose gel. The yield of joint molecules (D-loops) was plotted as a graph. Experiments were repeated at least three times; error bars represent S. D.

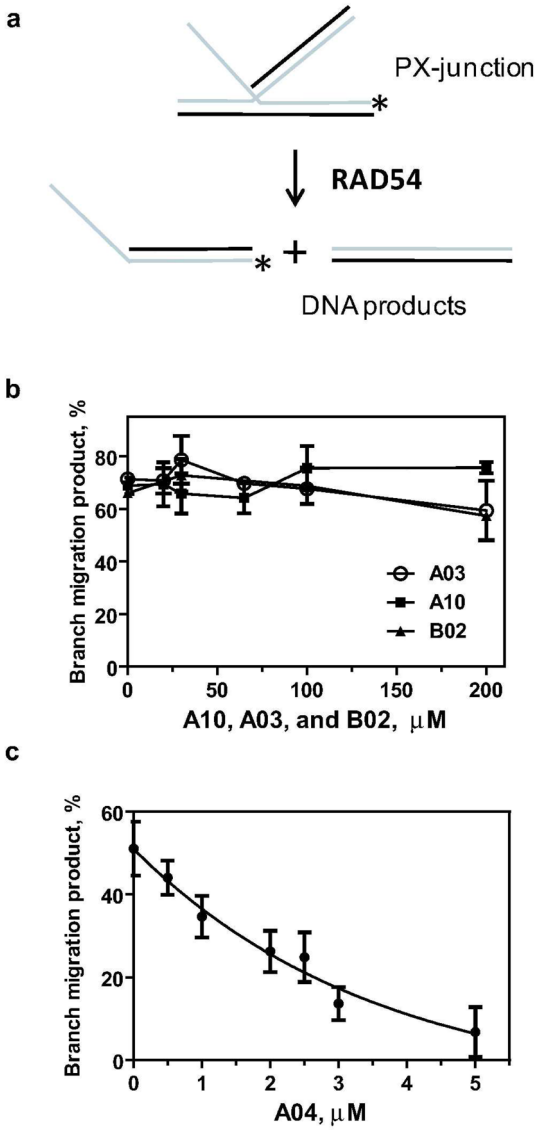

Figure 6. The effect of A03, A04, A10 and B02 compounds on branch migration activity of RAD54

(A) The scheme of branch migration promoted by RAD54. The asterisk denotes the ^{32}P label. (B) and (C) Branch migration was initiated by adding RAD54 (100 nM) to the mixtures containing PX-junctions (33 nM, molecules) and the small molecule inhibitors (in indicated concentrations). DNA products were analyzed by electrophoresis in 8% polyacrylamide gels. For each inhibitor concentration, the extent of branch migration was determined after 5 min of reaction (linear phase). The results are presented as a graph. Experiments were repeated at least three times; error bars represent S.D.

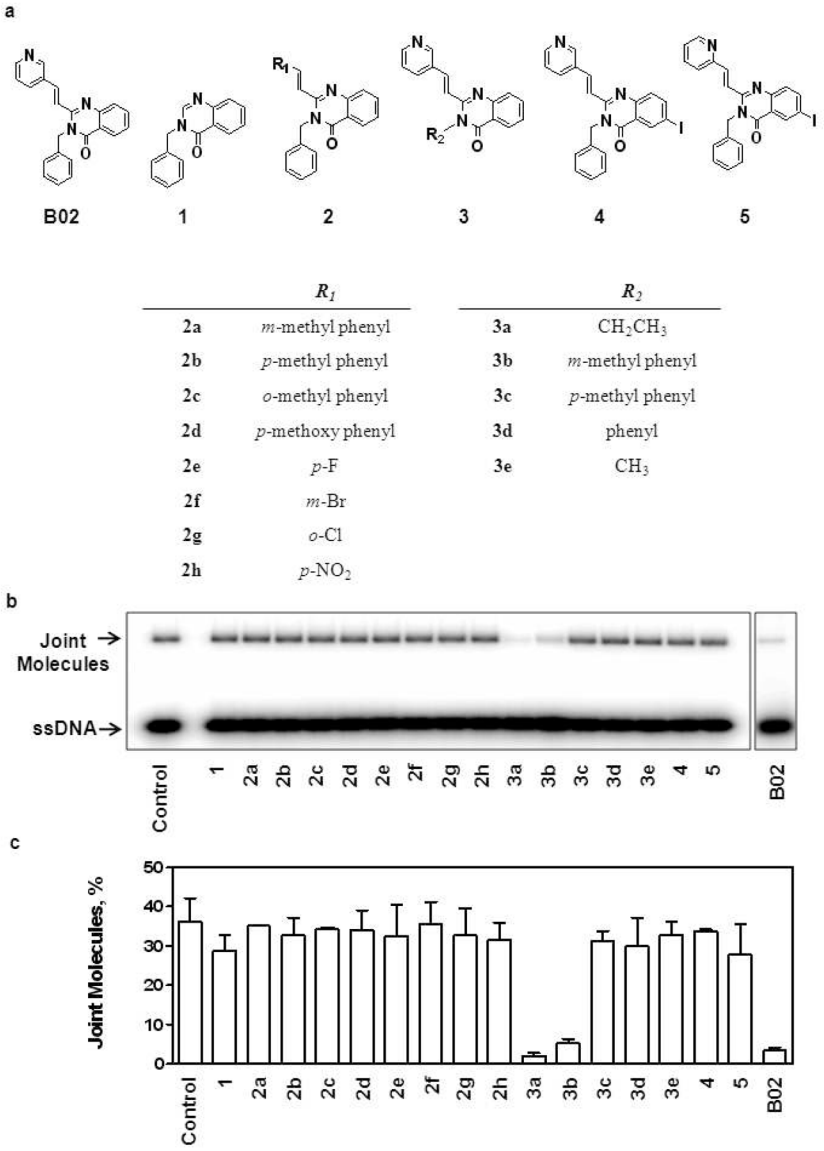

	R_1		R_2
2a	*m*-methyl phenyl	**3a**	CH_2CH_3
2b	*p*-methyl phenyl	**3b**	*m*-methyl phenyl
2c	*o*-methyl phenyl	**3c**	*p*-methyl phenyl
2d	*p*-methoxy phenyl	**3d**	phenyl
2e	*p*-F	**3e**	CH_3
2f	*m*-Br		
2g	*o*-Cl		
2h	*p*-NO_2		

Figure 7. Analysis of Structure-Activity Relationship (SAR) of B02 compound

(A) The structures of **B02** and its derivatives. (B) The effect of indicated **B02** derivatives on D-loop formation by RAD51. RAD51 (1 μM) was incubated with a 90-mer ssDNA (3 μM) (Oligo 90) for 15 min followed by addition of indicated compounds (50 μM). After a 30-min incubation, the D-loop formation was initiated by addition of 50 μM supecoiled pUC19 dsDNA. The DNA products were analyzed by electrophoresis in a 1% agarose gel. The control reaction was performed under the identical conditions, except that no tested compounds were added. (C) The yield of joint molecules (D-loops) was plotted as a graph. Experiments were repeated at least three times; error bars represent S.D.

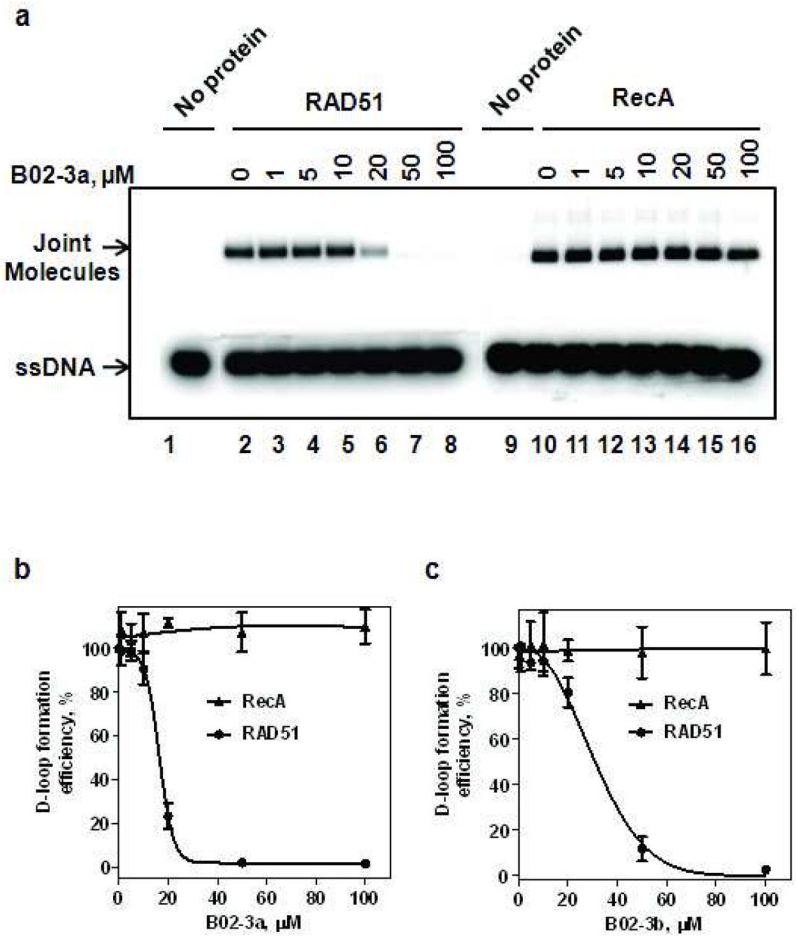

Figure 8. Effect of B02-3a and B02-3b compounds on DNA strand exchange activity of RAD51 and RecA

A) The effect of **B02-3a** on the DNA strand exchange activity of RAD51 and RecA. The nucleoprotein filaments were formed by incubating RAD51 (1 μM) or RecA (1 μM) with ssDNA (3 μM), then **B02-3a** was added in indicated concentrations and incubation continued for 30 min. D-loop formation was initiated by addition of pUC19 supercoiled dsDNA (50 μM). The DNA products were analyzed by electrophoresis in a 1% agarose gel. (B) The data from (A) was plotted as a graph. The yield of D-loop formation in the absence of **B02-3a** was expressed as 100%; the actual yield was 45.1 % and 34.2%, for RecA and RAD51, respectively. (C) The effect of **B02-3b** on the DNA strand exchange activity of RAD51 and RecA. The reactions were carried out as in A; the data are plotted as a graph. The yield of D-loop formation in the absence of **B02-3b** was expressed as 100%; the actual yield was 48.1 % and 31.6%, for RecA and RAD51, respectively. Experiments were repeated at least three times; error bars represent S.D.